Cite this: *INEOS OPEN*, **2025**, *8 (1–3)*, XX–XX
DOI: 10.32931/ioXXXXx

Received XX Month 20XX,
Accepted 20 January 2025

http://ineosopen.org

EFFICIENT IN-MAGNET ^{15}N HYPERPOLARIZATION INDUCED BY REVERSIBLE EXCHANGE OF PARAHYDROGEN WITH AN Ir-BASED CATALYST

D. A. Markelov,*[a,b] A. S. Kiryutin,[a] I. D. Kosenko,[c] Zh. V. Matsulevich,[d] I. A. Godovikov,[c] and A. V. Yurkovskaya[a]

[a] *International Tomography Center, Siberian Branch of the Russian Academy of Sciences, ul. Institutskaya 3A, Novosibirsk, 630090 Russia*
[b] *Novosibirsk State University, ul. Pirogova 1, Novosibirsk, 630090 Russia*
[c] *Nesmeyanov Institute of Organoelement Compounds, Russian Academy of Sciences, ul. Vavilova 28, str. 1, Moscow, 119334 Russia*
[d] *Nizhny Novgorod State Technical University, ul. Minina 24, Nizhny Novgorod, 603155 Russia*

Abstract

Nuclear magnetic resonance (NMR) suffers from its low sensitivity which can be dramatically increased by the nuclear spin hyperpolarization. Signal amplification by reversible exchange (SABRE) is a hyperpolarization technique based on the rational usage of parahydrogen as a source of hyperpolarization. This work reports in-magnet ^{15}N polarization (0.47%) of 3-methyl-[1,2,4]-selenadiazolo-[4,5-a]-pyridin-4-ium bromide (SDAP) and its ^{77}Se satellites obtained by the SABRE with RF excitation of ^{1}H and ^{15}N nuclear spins.

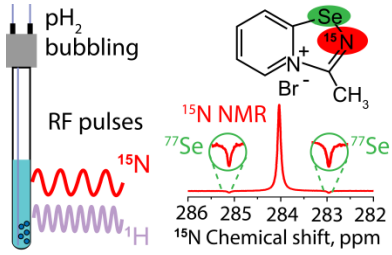

Key words: heteronuclear NMR, spin hyperpolarization, parahydrogen, SABRE.

Introduction

In the majority of cases, NMR operates with the thermal ensemble of nuclear spins, which results in weak NMR signals. This occurs since thermal nuclear magnetization typically has a low value, as it is proportional to the population imbalance between the nuclear spin energy levels at equilibrium. Nuclear spin hyperpolarization is based on the preparation of the nuclear spin order which is far from equilibrium at a given temperature and therefore provides an efficient solution to the problem of improving the NMR sensitivity.

Parahydrogen-induced polarization (PHIP) [1] is a hyperpolarization technique which employs parahydrogen (pH_2) as a non-equilibrium source of nuclear polarization. Parahydrogen itself does not contribute to the NMR signal, as it is a spin isomer of molecular hydrogen with the total nuclear spin of zero. However, if the symmetry between pH_2 protons is broken, its spin order can be transferred into polarization of a target molecule. In the classical (hydrogenative) version of PHIP, a substrate with unsaturated bonds is hydrogenated by parahydrogen in the presence of a catalyst. This, in turn, results in a strong enhancement of the ^{1}H NMR signals of the pH_2-nascent protons in the target molecule. This polarization of protons can be transferred to other nuclei of the molecule [2].

In recent years, a non-hydrogenative version of PHIP has been actively developed, which is termed the signal amplification by reversible exchange (SABRE) [3]. In SABRE, parahydrogen is not permanently incorporated into a target molecule. Instead, parahydrogen and a substrate molecule form a transient polarization transfer complex at an Ir-based catalyst, as demonstrated in Fig. 1a.

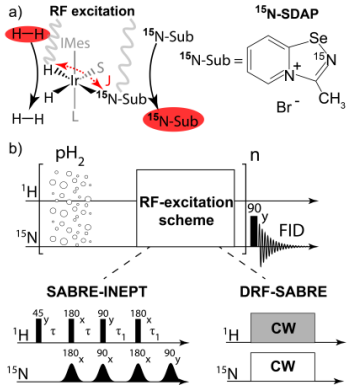

Figure 1. Scheme of the SABRE polarization transfer in a high magnetic field. (***a***) Reversible exchange of parahydrogen and substrate molecules, ^{15}N-Sub, with Ir-Imes complex (left) and the structure of the substrate to-be-polarized, 3-methyl-[1,2,4]-selenadiazolo-[4,5-a]-pyridin-4-ium bromide (^{15}N-SDAP) (right). (***b***) Upper line: an experimental protocol for the polarization transfer; lower line: (left) SABRE-INEPT pulse sequence with non-selective high-power RF-pulses, (right) DRF-SABRE pulse sequence with selective low-power CW pulses applied simultaneously in double resonance with respect to the interacting ^{1}H and ^{15}N nuclei in the complex.

The polarization transfer from parahydrogen to the substrate then occurs during their transient bonding to the complex. More precisely, it is coherently driven by a scalar J-coupling interaction of the nuclear spins in the polarization transfer complex. As the substrate participates in the reversible exchange, it acquires polarization in a continuous manner without a chemical modification. This makes SABRE a highly promising candidate for the hyperpolarization of nuclear spins in biomolecules. SABRE reveals its potential when applied to the

biologically relevant heteronuclei with a spin of $\frac{1}{2}$, *e.g.*, ^{13}C, ^{15}N, *etc*. This is because these nuclei have long relaxation times and therefore are considered as reservoirs for the long-term storage of polarization [4]. Hyperpolarized heteronuclear spins provide unique possibilities for studying metabolic processes *in vivo* [5].

However, the heteronuclear SABRE polarization transfer occurs only if spin dynamics in the polarization transfer complex is correctly optimized. This, in turn, requires the usage of external polarizers: sophisticated devices providing optimal conditions for the polarization transfer. Typically, a polarizer contains multilayer magnetic shields compensating the magnetic field of the Earth and providing a zone with an ultralow magnetic field (<1 μT). Demand for the external polarizers to hyperpolarize heteronuclear spins remains a challenge for the common experimental implementation of SABRE. Radiofrequency (RF) excitation of nuclear spins allows for avoiding this limitation and enabling the performance of SABRE inside a high magnetic field of the NMR spectrometer [6]. The in-magnet SABRE hyperpolarization is complicated, because it requires a design of the RF excitation scheme and precise experimental optimization of the RF fields. For the in-magnet hyperpolarization, we used two different pulse sequences, as shown in Fig. 1b. The first pulse sequence is termed SABRE-INEPT (INEPT, insensitive nuclei enhanced by polarization transfer) [7], which is considered as a standard approach for the SABRE hyperpolarization. As an alternative approach for the in-magnet hyperpolarization, we used DRF-SABRE pulse sequence (DRF, double radiofrequency), which has been recently proposed by us [8]. In this work, we demonstrate the in-magnet SABRE hyperpolarization of ^{15}N nuclei in ^{15}N-labelled 3-methyl-[1,2,4]-selenadiazolo-[4,5-a]-pyridin-4-ium bromide (^{15}N-SDAP), a compound belonging to the class of selenadiazoles which exhibit potential antimicrobial and antitumor activity [9]. To reveal the full potential of the in-magnet SABRE for biologically relevant molecules, we compare the efficiency of the hyperpolarization of ^{15}N-SDAP obtained by the standard (SABRE-INEPT) and novel (DRF-SABRE) approaches.

Experimental section

We used [IrCl(COD)(IMes)] as a precatalyst for the polarization transfer complex (IMes = 1,3-bis(2,4,6-trimethylphenyl)imidazol-2-ylidene, COD = cyclooctadiene), ^{15}N-SDAP as a substrate for hyperpolarization, and DMSO (dimethyl sulfoxide) as a stabilizing co-substrate [10]. The investigated sample consisted of ^{15}N-SDAP (18 mM), DMSO (650 mM), and [IrCl(COD)(IMes)] (4 mM) dissolved in 600 μL of CD_3OD. [IrCl(COD)(IMes)] was synthesized according to the standard procedure [11], ^{15}N-SDAP was synthesized according to the procedure described elsewhere [12], where, at the final stage, ^{15}N-labeled acetonitrile (98% Atom, Sigma 487864) was used. Methanol-d_4 was purchased from Carl Roth, DMSO was purchased from Sigma-Aldrich. All experiments were conducted at a 400 MHz NMR spectrometer with a magnetic field of 9.4 T. For parahydrogen bubbling, we used an automated gas-flow system [13]. Parahydrogen bubbling pressure was equal to 4 atm. To determine the enhancement of the ^{15}N NMR signal quantitively, we used the following formula

$$\boldsymbol{\varepsilon} = \frac{[\boldsymbol{S_{ref}}]\boldsymbol{I}}{[\boldsymbol{S}]\boldsymbol{I}_{\boldsymbol{ref}}^{\boldsymbol{th}}}, \quad (1)$$

where $\boldsymbol{\varepsilon}$ is the ^{15}N signal enhancement, $\boldsymbol{I}$ is the integral intensity of the hyperpolarized ^{15}N NMR signal, $[\boldsymbol{S}]$ is a concentration of the ^{15}N substrate to-be-polarized, $\boldsymbol{I}_{\boldsymbol{ref}}^{\boldsymbol{th}}$ is the integral intensity of the ^{15}N NMR signal of the thermal reference, $[\boldsymbol{S_{ref}}]$ is the concentration of the ^{15}N substrate in the thermal reference sample.

Results and discussion

The first step of our experiments was the precatalyst activation [14]. It consisted in bubbling the sample containing the precatalyst with parahydrogen. During this process, an active polarization transfer complex was formed from [IrCl(COD)(IMes)], which was manifested in the appearance of signals in the hydride region of the ^{1}H NMR spectrum. After this, the high-field SABRE pulse sequences can be applied to hyperpolarize the nuclear spins (see Fig. 1b). The protocol of the experiments consisted of the polarization transfer cycles from parahydrogen to the substrate repeated consequently *n* times (in our experiments *n* = 30). Each cycle consists of fast bubbling the sample with parahydrogen (within 0.5 s) followed by a time delay introduced to remove the bubbles from the sample (0.5 s), and RF excitation of the nuclear spins aimed at inducing the longitudinal component of the ^{15}N polarization. This method of bubbling in a burst mode, on the one hand, allows for saturating the solution with fresh parahydrogen. On the other hand, it allows applying RF pulses in conditions of high magnetic field homogeneity. The ^{15}N polarization of the substrate is generated in the SABRE complex and then transferred to the free substrate in bulk *via* the reversible chemical exchange. As the final step, the non-equilibrium longitudinal component of the substrate magnetization was detected by 90-pulse followed by the free induction decay (FID) recording. The optimal choice of the RF excitation scheme is the most important for the hyperpolarization. Thus, SABRE-INEPT pulse sequence generates ^{15}N magnetization of the substrate *via* a certain combination of the ^{1}H and ^{15}N RF pulses separated by the time delays: τ and τ_1. For the ^{15}N polarization transfer, τ and τ_1 have to be correctly adjusted (we used τ = 8.5 ms and τ_1 = 10 ms). In turn, DRF-SABRE is based on the selective RF excitation of the complex-bound nuclei with weak continuous-wave (CW) ^{1}H and ^{15}N fields (we used the CW field amplitudes of 8 Hz). The ^{1}H CW field selectively excites the hydride proton in its trans-position with respect to the complex-bound substrate, where the strongest *J*-coupling is present (see Fig. 1a). For efficient DRF-SABRE performance, the frequencies of the CW fields have to be accurately optimized (we used ^{1}H CW with –23.72 ppm and ^{15}N CW with 241.87 ppm frequencies).

Figure 2 demonstrates the single-scan ^{15}N (^{1}H decoupled) NMR spectra of ^{15}N-SDAP hyperpolarized by the in-magnet SABRE pulse-sequences: (***a***) SABRE-INEPT, (***b***) DRF-SABRE. Figure 2c demonstrates the thermal signal of the reference sample, 500 mM of ^{15}N-labelled pyridine. Enhancements, $\boldsymbol{\varepsilon}$, of the hyperpolarized ^{15}N NMR signals relative to the thermal reference signal were calculated using equation 1 and are demonstrated in each subplot. It should be noted that hyperpolarized ^{77}Se satellites (7.6% of the natural abundance)

with the splitting of 87 Hz are also observed in the ^{15}N spectra. It is noteworthy that that DRF-SABRE ($\boldsymbol{\varepsilon = -1400}$) is 4.7 times more efficient than SABRE-INEPT ($\boldsymbol{\varepsilon = -300}$) for the ^{15}N hyperpolarization of ^{15}N-SDAP and 2.5 times more efficient for the ^{15}N hyperpolarization of its ^{77}Se satellites ($\boldsymbol{\varepsilon = 290}$ and $\boldsymbol{\varepsilon = -115}$ for DRF-SABRE and SABRE-INEPT respectively).

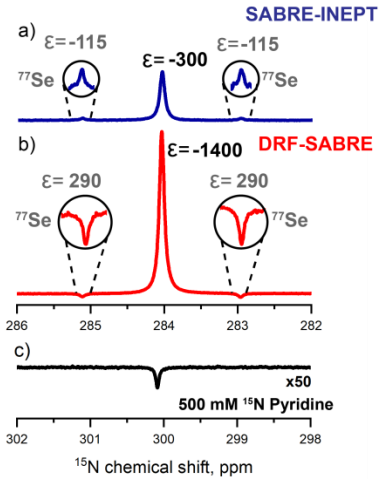

Figure 2. Hyperpolarized ^{15}N (^{1}H decoupled) spectra of ^{15}N-SDAP (18 mM) obtained with two pulse sequences: SABRE-INEPT (***a***), DRF-SABRE (***b***). ^{15}N NMR spectrum of ^{15}N-pyridine (500 mM) in methanol-d_4 at thermal equilibrium detected at 9.4 T (multiplied by the factor of 50 on the vertical axis) (***c***). This signal was used as a reference for the calculation of the NMR enhancement of the ^{15}N signals, denoted by ε. The hyperpolarized ^{77}Se satellites in (***a***) and (***b***) are shown enlarged in the circles above the corresponding signals. The temperature of the samples was reduced to 15 °C.

Thus, the highest value of the ^{15}N signal enhancement for ^{15}N-SDAP was obtained by the DRF-SABRE pulse sequence ($\boldsymbol{\varepsilon = -1400}$, which corresponds to 0.47% of the ^{15}N polarization). This is in good agreement with our recent work, where DRF-SABRE was demonstrated to be more efficient than other pulse sequences [8]. Such levels of heteronuclear polarization are comparable with the largest ones that can be potentially achieved by the high-field SABRE methods ($\boldsymbol{\varepsilon \approx 2500}$) [7, 8]. Moreover, in our work we demonstrated that DRF-SABRE can be exploited to hyperpolarize the nuclear spins in a complex spin systems containing several types of heteronuclei, in our case, ^{15}N and ^{77}Se, paving the road for the high-field hyperpolarization of a broader range of magnetic nuclear isotopes and molecules.

Conclusions

Acknowledgements

This work was supported by the Russian Science Foundation (project no. 23-73-10103).

Corresponding author

* E-mail: d.markelov@tomo.nsc.ru (D. A. Markelov).

Electronic supplementary information

Electronic supplementary information (ESI) available online: the optimization data of the SABRE pulse sequences and ^{1}H NMR spectra of the catalyst activation. For ESI, see DOI: 10.32931/ioXXXXx.

References

1. C. R. Bowers, D. P. Weitekamp, *J. Am. Chem. Soc.*, **1987**, *109*, 5541–5542. DOI: 10.1021/ja00252a049
2. G. Buntkowsky, F. Theiss, J. Lins, Y. A. Miloslavina, L. Wienands, A. Kiryutin, A. Yurkovskaya, *RSC Adv.*, **2022**, *12*, 12477–12506. DOI: 10.1039/D2RA01346K
3. R. W. Adams, J. A. Aguilar, K. D. Atkinson, M. J. Cowley, P. I. P. Elliott, S. B. Duckett, G. G. R. Green, I. G. Khazal, J. López-Serrano, D. C. Williamson, *Science*, **2009**, *323*, 1708–1711. DOI: 10.1126/science.1168877
4. A. S. Kiryutin, V. P. Kozinenko, A. V. Yurkovskaya, *ChemPhotoChem*, **2024**, *8*, e202300151 DOI: 10.1002/cptc.202300151
5. A. B. Schmidt, E. Y. Chekmenev, H. de Maissin, P. R. Groß, S. Petersen, L. Nagel, F. Schilling, I. Schwartz, T. Reinheckel, J.-B. Hövener, S. Knecht, *Analysis Sensing*, **2024**, e202400039. DOI: 10.1002/anse.202400039
6. T. Theis, M. Truong, A. M. Coffey, E. Y. Chekmenev, W. S. Warren, *J. Magn. Reson.*, **2014**, *248*, 23–26. DOI: 10.1016/j.jmr.2014.09.005
7. S. Knecht, A. S. Kiryutin, A. V. Yurkovskaya, K. L. Ivanov, *J. Magn. Reson.*, **2018**, *287*, 10–14. DOI: 10.1016/j.jmr.2017.12.010
8. D. A. Markelov, V. P. Kozinenko, A. S. Kiryutin, A. V. Yurkovskaya, *J. Chem. Phys.*, **2024**, *161*, 214203. DOI: 10.1063/5.0236841
9. A. C. Ruberte, C. Sanmartin, C. Aydillo, A. K. Sharma, D. Plano, *J. Med. Chem.*, **2020**, *63*, 1473–1489. DOI: 10.1021/acs.jmedchem.9b01152
10. W. Iali, S. S. Roy, B. J. Tickner, F. Ahwal, A. J. Kennerley, S. B. Duckett, *Angew. Chem., Int. Ed.*, **2019**, *58*, 10271–10275. DOI: 10.1002/anie.201905483
11. I. Kownacki, M. Kubicki, K. Szubert, B. Marciniec, *J. Organomet. Chem.*, **2008**, *693*, 321–328. DOI: 10.1016/j.jorganchem.2007.11.013
12. V. N. Khrustalev, M. M. Grishina, Z. V. Matsulevich, J. M. Lukiyanova, G. N. Borisova, V. K. Osmanov, A. S. Novikov, A. A. Kirichuk, A. V. Borisov, E. Solari, A. G. Tskhovrebov, *Dalton Trans.*, **2021**, *50*, 10689–10691. DOI: 10.1039/D1DT01322J
13. A. S. Kiryutin, G. Sauer, S. Hadjiali, A. V. Yurkovskaya, H. Breitzke, G. Buntkowsky, *J. Magn. Reson.*, **2017**, *285*, 26–36. DOI: 10.1016/j.jmr.2017.10.007
14. M. L. Truong, F. Shi, P. He, B. Yuan, K. N. Plunkett, A. M. Coffey, R. V. Shchepin, D. A. Barskiy, K. V. Kovtunov, I. V. Koptyug, K. W. Waddell, B. M. Goodson, E. Y. Chekmenev, *J. Phys. Chem. B*, **2014**, *118*, 13882–13889. DOI: 10.1021/Jp510825b